Archives of Toxicology (2023) 97:405–420
https://doi.org/10.1007/s00204-022-03415-x

INORGANIC COMPOUNDS

Silver nanoparticles exert toxic effects in human monocytes and macrophages associated with the disruption of Δψm and release of pro-inflammatory cytokines

Adelaide Sousa[1] · Ana T. Rufino[1] · Rui Fernandes[2] · Ana Malheiro[2] · Félix Carvalho[3,4] · Eduarda Fernandes[1] · Marisa Freitas[1]

Received: 29 July 2022 / Accepted: 3 November 2022 / Published online: 24 November 2022

Abstract

Silver nanoparticles (AgNP) are the most widely produced type of nanoparticles due to their antimicrobial and preservative properties. However, their systemic bioavailability may be considered a potential hazard. When AgNP reach the bloodstream, they interact with the immune cells, contributing to the onset and development of an inflammatory response. Monocytes and macrophages play a pivotal role in our defense system, but the interaction of AgNP with these cells is still not clear. Therefore, the main objective of this work was to assess the cytotoxic and pro-inflammatory effects induced by 5, 10, and 50 nm AgNP coated with polyvinylpyrrolidone (PVP) and citrate, in concentrations that could be attained in vivo (0–25 µg/mL), in human monocytes isolated from human blood and human macrophages derived from a monocytic cell line (THP-1). The effects of PVP and citrate-coated AgNP on cell viability, mitochondrial membrane potential, and cytokines release were evaluated. The results evidenced that AgNP exert strong harmful effects in both monocytes and macrophages, through the establishment of a strong pro-inflammatory response that culminates in cell death. The observed effects were dependent on the AgNP concentration, size and coating, being observed more pronounced cytotoxic effects with smaller PVP coated AgNP. The results showed that human monocytes seem to be more sensitive to AgNP exposure than human macrophages. Considering the increased daily use of AgNP, it is imperative to further explore the adverse outcomes and mechanistic pathways leading to AgNP-induced pro-inflammatory effects to deep insight into the molecular mechanism involved in this effect.

Keywords Silver nanoparticles · Inflammation · Human monocytes · Human macrophages · Toxicity

✉ Eduarda Fernandes
egracas@ff.up.pt

✉ Marisa Freitas
marisafreitas@ff.up.pt

1 LAQV, REQUIMTE, Laboratory of Applied Chemistry, Department of Chemical Sciences, Faculty of Pharmacy, University of Porto, Rua de Jorge Viterbo Ferreira No. 228, 4050-313 Porto, Portugal

2 Histology and Electron Microscopy (HEMS), Instituto de Investigação e Inovação em Saúde i3S, Instituto de Biologia Molecular e Celular BMC, Universidade Do Porto, Porto, Portugal

3 UCIBIO, REQUIMTE, Laboratory of Toxicology, Department of Biological Sciences, Faculty of Pharmacy, University of Porto, 4050-313 Porto, Portugal

4 Associate Laboratory i4HB - Institute for Health and Bioeconomy, Faculty of Pharmacy, University of Porto, Porto, Portugal

Introduction

Nanoscience and nanotechnology are rapidly evolving complementary fields of research and industrial innovation, being widely applied in our daily life, with several potential applications in different areas as agriculture, medicine, engineering, pharmaceutical sciences, and food industry (Martirosyan et al. 2012). The unique physicochemical and biological properties of silver nanoparticles (AgNP) make them the most widely produced (about 55 tons per year) and commercialized nanoparticles (NP), accounting with more than 400 consumer products, which represents 51% of the consumer products based in nanomaterials (Ducheyne 2017). AgNP have been largely used in several application areas, including health and fitness (e.g., clothing, cosmetics, filtration, personal care, sporting goods, sunscreen), home and garden (e.g. cleaning, construction materials, home furnishings, luggage, paint, pets), food and beverage (e.g.

cooking, food, storage and supplements), children's basics and toys, electronics, computers, and others (Fauss 2008; Council 2012).

To improve the shelf life and safety of food products, the direct or indirect incorporation of AgNP in food industry has been increasing exponentially, from cultivation to production, including processing and packaging. Addition of AgNP into food products may improve their antibacterial properties, as well as the mechanical properties of their packages (by enhancing the strength of nanofilms) (Berekaa 2015). Although the majority of AgNP used in food industry remain bound to the food packaging materials, it is possible that some of these AgNP migrate from these containers into foods, being, consequently, ingested (Berekaa 2015; McClements and Xiao 2017; Pathakoti et al. 2017). This frequent contact with AgNP together with their ultra-small sizes may result in the increase of their bioavailability and systemic exposure (Zorraquín-Peña et al. 2020). The human dietary intake of silver (Ag), resulting from the widespread use of AgNP, was estimated to be 70–90 µg/day (Zorraquín-Peña et al. 2020). However, considering the increased use of these metal NP in the food industry, it is expected to observe a dramatic increase in the exposure values (Mathur et al. 2018; Zorraquín-Peña et al. 2020). AgNP have already been considered by the U.S. Environmental Protection Agency (US EPA) as an environmental hazard and pollutant in natural waters, partly due to its persistence in the environment, bio-accumulative features and its high toxicity to life forms (NanoComposix 2004, (HERO) 2022). Following absorption, AgNP reach the bloodstream, and interact with the "guard cells" of the immune system, potentially modulating their activity and activating an inflammatory response (Galdiero et al. 2011; Arora et al. 2012; Haase et al. 2014).

Monocytes and macrophages are important components of mononuclear phagocyte system, participating in the innate immunity. These cells are not only involved in the initiation, development and resolution of inflammation, but also play an important role as immunomodulatory and immunoregenerative systems (Chiu and Bharat 2016). Despite their important role in the defense of the organism, during a prolonged exposure to a stimuli, the excessive activity of these cells can contribute to the perpetuation of the inflammatory responses, which could culminate in a chronic condition (Chiu and Bharat 2016).

Therefore, considering the increased and inevitable human exposure to AgNP, it is of utmost importance to extensively evaluate their potential effects on these immune cells. It is currently accepted that physicochemical properties of AgNP influence their interaction with the cells (Ferdous and Nemmar 2020). Although it is agreed that particle size is likely to contribute to AgNP cytotoxicity, the coating agents used to stabilize and maintain their specific characteristics can also be also responsible for some immunogenic properties (Huang et al. 2017). Two commonly used coating agents are citrate and polyvinylpyrrolidone (PVP), which impart a negative charge, giving AgNP a wide appeal for manufacturing and consumer use (de Lima et al. 2012). Several studies reported the AgNP' role in the induction of an immunologic response, through the activation of monocytes and macrophages (Chan et al. 2015; Kononenko et al. 2015; Ferdous and Nemmar 2020). However, to the best of our knowledge, there are no studies in the literature comparing the pro-inflammatory and cytotoxic effects of AgNP of several sizes and coated with different agents, using monocytes and macrophages.

Therefore, the main objective of this work was to evaluate the cytotoxic and pro-inflammatory effects of AgNP with three different sizes (5, 10 and 50 nm) and two different coating agents, PVP and citrate, in human monocytes isolated from human blood and human macrophages derived from a monocytic cell line (THP-1). To achieve this goal, the effects of AgNP on cell viability, mitochondrial membrane potential, and cytokines release were evaluated.

Materials and methods

Materials

All solvents and chemicals were of analytical grade. BioPure PVP and citrate coated-AgNP (5, 10 and 50 nm) were obtained from nanoComposix (San Diego, CA). Dimethyl sulfoxide (DMSO), 3-(4,5-dimethylthiazol-2-yl)-2,5-diphenyltetrazolium (MTT), carbonyl cyanide chlorophenylhydrazone (CCCP), lipopolysaccharide (LPS), Dulbecco′s phosphate buffered saline (PBS) without calcium chloride ($CaCl_2$) and magnesium chloride, D-glucose, heat-inactivated fetal bovine serum (FBS), histopaque 1077 and 1119, $CaCl_2$, Trizma-base®, magnesium sulfate ($MgSO_4$), trypan blue solution 0.4%, phorbol 12-myristate 13-acetate (PMA) and RPMI 1640 medium were obtained from Sigma-Aldrich (St. Louis, MO, USA). The antibody CD11b, the commercial FITC Annexin V Apoptosis Detection Kit I, Mitoscreen (JC-1) Kit and BD Cytometric Bead Array (CBA) Human Inflammatory Cytokines Kit® were obtained from BD Biosciences (New Jersey, USA).

Methods

TEM analysis: AgNP characterization and cell ultrastructure

(a) AgNP characterization

The manufacturer characterized each batch within their solvent (aqueous 2 mM citrate for 5, 10 and 50 nm citrate coated-AgNP and milli-Q water for 5, 10 and 50 nm PVP-coated AgNP) by transmission electron microscopy (TEM)

to determine size and shape distributions, UV–visible spectroscopy to measure the optical properties, dynamic light scattering to determine particle hydrodynamic diameter, and zeta potential measurement to determine particle surface charge. BioPure nanoparticles are extensively washed with the suspending solvent to remove residual reactants from the manufacturing process. Mass concentration was determined with inductively coupled plasma mass spectroscopy (ICP-MS). The particles were sterile filtered and tested for endotoxin contamination before delivery. Throughout the study, nanomaterials were stored at 4 °C.

The characterization of citrate and PVP-coated AgNP, diluted in RPMI medium supplemented 10% (v/v) heat-inactivated FBS, in the culture medium used in the following assays, was also performed by TEM, to predict possible size and morphology modifications. Samples of different AgNP concentrations were placed on a glow-discharged carbon-coated collodion film supported on 300-mesh copper grids and left to stand for 10 min. Excess solution was then removed and AgNP were analyzed using a JEOL JEM 1400 Electron Microscope electron microscope operating at 80 kV and equipped with an Orius (Gatan) camera interface.

(b) Cell ultrastructure

For the ultrastructure analysis, cells were fixed in a solution of 2.5% (v/v) glutaraldehyde (#16316; Electron Microscopy sciences) with 2.0% (v/v) formaldehyde (#15713; Electron Microscopy sciences) in 0.1 M sodium cacodylate buffer (pH 7.4) for 1 h, at room temperature (RT), and post fixed in 1% (v/v) osmium tetroxide (#19190; Electron Microscopy Sciences) diluted in 0.1 M sodium cacodylate buffer. After centrifugation, the pellet was resuspended in HistogelTM (Thermo, HG-4000–012) and then stained with aqueous 1% (v/v) uranyl acetate solution overnight, dehydrated and embedded in Embed-812 resin (#14120; Electron Microscopy sciences). Ultra-thin sections (50 nm thickness) were cut on a RMC Ultramicrotome (PowerTome, USA) using Diatome diamond knifes, mounted on mesh copper grids (Electron Microscopy Sciences), and stained with uranyl acetate substitute (#22409; Electron Microscopy Sciences) and lead citrate (#22410 Electron Microscopy Sciences) for 5 min each. Samples were viewed on a JEOL JEM 1400 transmission electron microscope (JEOL, Tokyo, Japan) and images were digitally recorded using a CCD digital camera Orius 1100 W (Gatan, USA) and further analyzed with the ImageJ® software (NIH, USA). The transmission electronic microscopy was performed at the HEMS core facility at i3S, University of Porto, Portugal.

Cell culture

THP-1 cells (ATCC® TIB-202TM) were purchased from the American Type Culture Collection and cultured according to their specific indications, using an RPMI medium supplemented 10% (v/v) heat-inactivated FBS, 2 mM of glutamine, 100 U/mL penicillin and 100 µg/mL streptomycin, in suspension, in a Haier CO_2 incubator (model HCP-168) at 37 °C in a humidified atmosphere of 95% (v/v) air and 5% (v/v) CO_2. During the experiments, cells were monitored by microscopic (Motic AE2000) observation to detect any morphological change and cell viability was thoroughly monitored by the trypan blue exclusion method. During the incubation periods, cells were maintained at 37 °C, in a humidified 5% (v/v) CO_2 atmosphere.

Differentiation of monocytic THP-1 cells into macrophagic THP-1 cells Considering the dataset available in the literature, THP-1 cells in culture medium were differentiated into macrophage-like cells (THP-1 macrophages) prior to each study (Ozleyen et al. 2021). To induce the differentiation of THP-1 monocytes into macrophages, cells were seeded in 96 or 48 well plates, at the desired cell density (0.5×10^6 to 2.2×10^6 cells/mL), and were exposed to PMA (80 nM), for 24 h. After this period, cells were washed in non-supplemented RPMI medium and incubated in fresh medium, without PMA, for 24 h. It is expected that differentiated cells are adherent, have lower rates of proliferation, are more phagocytic, and generally have increased cell surface expression of CD11b (Mittar et al. 2011; Lai et al. 2021). Therefore, to confirm the differentiation process, the expression of CD11b marker was analyzed in the THP-1 differentiated cells, by flow cytometry. Briefly, after the differentiation process, cell supernatants were discarded, and cells were washed with PBS buffer and detached from cells plates with trypsin:EDTA solution. Afterwards, cells were centrifuged for 5 min at 200 g, the supernatant was discarded, and the resulting pellet was resuspended in PBS. Therefore, cells were incubated at RT for 30 min with CD11b fluorochrome-conjugated monoclonal antibody (50 µg/mL). Subsequently, cells were washed with PBS and centrifuged for 5 min at 300 g and the supernatant was discarded. PBS was added to the resulting pellet and fluorescence signals for, at least, 10.000 events were immediately read in logarithmic mode in an Accuri C6 flow cytometer (BD, Becton, Dickinson and Company, USA). The data obtained were analyzed using C Flow (Accuri) software. Fluorescence due to CD11b fluorochrome-conjugated monoclonal antibody was followed in channel 4 (FL4).

Isolation of human monocytes

All patient-related procedures and protocols were performed in accordance with the Declaration of Helsinki and approved by the Ethic Committee of the Centro Hospitalar do Porto. After informed consent, venous blood was collected by antecubital venipuncture from each human healthy volunteer

(males and nonpregnant females, aged 18–65 years) into vacuum tubes with K_3EDTA for the monocytes isolation procedure. As previously reported by our research group (Freitas et al. 2008), the isolation of human monocytes was performed according to the density gradient centrifugation method. Briefly, the collected blood was added to a 15 mL polypropylene tube following the addition of 3 mL of histopaque 1119 and 3 mL of histopaque 1077 solutions. Subsequently, the tube was centrifuged at 900 g for 30 min at 20 °C. Then, the monocytes pellet was collected, and the volume was doubled using PBS. The resultant suspension was centrifuged at 850 g for 5 min at 4 °C, and the supernatant discarded. The monocytes pellet was resuspended in PBS, and this suspension was centrifuged at 850 g for 5 min at 4 °C, and the resulting supernatant was discarded. The monocytes pellet obtained was resuspended in tris-glucose buffer (25 mM Trizma®, 140 mM NaCl, 1.26 mM $CaCl_2$, 5.37 mM KCl, 0.81 mM $MgSO_4$, 5.5 mM D-glucose, pH 7.4). Cell viability and cell yield were determined by the trypan blue exclusion method, using a Neubauer chamber and an optic microscope (Nikon Eclipse E200). Cells were kept on ice under stirring conditions in an orbital shaker for approximately 1 h before performing the following assays.

Evaluation of cell viability after incubation with AgNP with Annexin V/Propidium Iodide

The evaluation of cell death was analyzed by flow cytometry, following simultaneous staining with propidium iodide (PI) and annexin V labelled with fluorescein isothiocyanate (FITC), according to a previously described method (Freitas et al. 2020), using the Annexin V-FITC Apoptosis Detection Kit. The externalization of phosphatidylserine as a marker of early-stage apoptosis was detected by the annexin V protein conjugated to FITC, whereas membrane damage due to late-stage apoptosis/necrosis was detected by the binding of PI to nuclear DNA. Briefly, human macrophages (1.1×10^5 cells/mL) or freshly isolated human monocytes (1.0×10^6 cells/mL) were seeded in 48 well plates and exposed to 5, 10 and 50 nm PVP and citrate coated-AgNP (0–25 µg/mL). Similarly, the cell death evaluation was also performed for the coating agents per se, namely, PVP and citrate (0.01 µg/mL) and Ag^+ (0.25 µg/mL). For human macrophages, after 24 h of exposure, cell supernatants were discarded, and cells were washed with PBS buffer and detached from cells plates with trypsin:EDTA solution. Concerning freshly isolated human monocytes, the exposure period was 2 h, and after this time, cells were transferred to adequate centrifugation tubes. Then, the two cell types were submitted to a centrifugation for 5 min at 400 g. The resulting pellet was washed in PBS and centrifuged, at the same conditions. The resulting supernatant was discarded, and PI and annexin V were added to the pellet. The resuspended mixture was incubated for 15 min in the dark, at RT. Finally, after incubation, 10 × diluted binding buffer was added. Samples were analyzed in an Accuri C6 flow cytometer (BD, Becton, Dickinson and Company, USA), and fluorescence signals, for at least 10.000 events for each sample, were collected in logarithmic mode and the data were analyzed using C Flow (Accuri) software. The green fluorescence due to annexin V conjugated with FITC was followed in channel 1 (FL1) and the fluorescence due to the PI was followed in channel 3 (FL3), and then a histogram of FL1 versus FL3 staining was plotted. The analysis was restricted to the monocytes and macrophages population, and for this purpose, a polygon gate was drawn according to their light scattering properties (in a forward versus side scatter plot), in which other blood cells and debris cells were excluded. Each study corresponded to, at least, three independent assays.

Assessment of mitochondrial membrane potential

The membrane-permeant JC-1 dye is widely used in apoptosis studies to monitor mitochondrial condition, since this dye exhibits membrane potential-dependent accumulation in mitochondria. The use of JC-1 dye, which fluoresces in the FL-1 channel and lacks fluorescence in the FL-2 channel, allows the monitoring of a possible mitochondrial depolarization, which is indicated by a concentration-dependent formation of red fluorescent J-aggregates that lead to a decrease in the red/green fluorescence intensity ratio.

The depolarization of $\Delta\psi m$ in human monocytes and macrophages induced by 5, 10 and 50 nm citrate and PVP-coated AgNP (0–25 µg/mL) and also of the coating agents per se, PVP and citrate (0.01 µg/mL) and Ag^+ (0.25 µg/mL) were evaluated, using the commercial flow cytometry detection kit (BD™ MitoScreen Flow Cytometry Mitochondrial Membrane Potential Detection Kit), according to manufacturer's instructions. Briefly, the human monocytes (2×10^6 cells/mL) or macrophages (1.1×10^5 cells/mL) were incubated with the positive control CCCP (0.1–200 µM) or with 5, 10 and 50 nm citrate and PVP-coated AgNP (0–25 µg/mL) during 2 h for monocytes and 16 and 24 h for macrophages. After this period, cells were collected and centrifuged, being then incubated with JC-1 Work solution for 15 min, at 37 °C, protected from light. After this period, cells were washed with assay buffer and centrifuged twice, at 400 g during 5 min, at RT. Lastly, the pellet was resuspended in the assay buffer and the alterations of the mitochondrial potential of the samples were analyzed in an Accuri C6 flow cytometer (BD, Becton, Dickinson and Company, USA), and fluorescence signals, for at least 10.000 events for each sample, were collected in logarithmic mode and the data were analyzed using C Flow (Accuri) software.

Detection and quantification of human inflammatory cytokines

The production of a set of cytokines [interleukin (IL)-8, IL-1β, IL-6, IL-10, tumor necrosis factor (TNF), and IL-12p70] was measured in the culture medium collected after the incubation of human monocytes or macrophages with positive control (LPS 1–4 μg/mL) or 5, 10 and 50 nm PVP and citrate-coated AgNP (0–25 μg/mL) for 2 or 24 h, respectively. Similarly, the cytokines production was also evaluated for the coating agents per se, PVP and citrate (0.01 μg/mL) and for Ag^+ (0.25 μg/mL). For this evaluation, it was used a flow cytometry detection kit [BD Cytometric Bead Array (CBA) Human Inflammatory Cytokines Kit®], following the manufacturer's instructions. This kit is based on the ability of beads with a known size and fluorescence, coated with antibodies specific for IL-8, IL-1β, IL-6, IL-10, TNF and IL-12p70 proteins to capture soluble analytes (cytokines), making it possible to detect analytes by flow cytometry. Briefly, the resultant culture medium was incubated with the mixed capture beads for 3 h, at RT, protected from the light. After this incubation period, wash buffer was added to each tube and centrifuged at 200 g for 5 min. The supernatant was then aspirated and discarded, and a wash buffer was added to the assay tubes for pellet resuspension. Samples were immediately processed in Accuri C6 flow cytometer (BD, Becton, Dickinson and Company, USA), using the red channel (FL3). Results were expressed as pg/mL of cytokines released in the media, as the mean ± SEM of, at least, three independent experiments.

Statistical analysis

All data are expressed as mean ± standard error of the mean deviation (SEM). The statistical analysis was performed using one-way analysis of variance (ANOVA), followed by Bonferroni's posthoc test, using GraphPad 6.01 software. For all comparisons, differences were considered statistically significant for a p-value of < 0.05.

Results

Characterization of AgNP

The assessment of AgNP physicochemical properties is essential, since they can affect their biodistribution, safety and efficacy and, consequently, their toxicity. The TEM images obtained for primary sizes, shape, and morphology of AgNP in water [images courtesy of the manufacturer, nanoComposix (San Diego, CA)] and in RPMI culture medium are represented in Fig. 1, with the corresponding statistical result represented in Table 1.

From the morphological point of view, the manufacturers reported that all the AgNP present in a spherical form in their origin solvents. It was not observed any significant differences in AgNP physicochemical characteristics using water *versus* RPMI culture medium, nor any effects on their aggregation state (Fig. 1).

No significant changes were observed in the average sizes of AgNP dispersed in RPMI when compared with the standard solvent, water, as it can be concluded from Table 1.

Evaluation of cell viability after incubation with AgNP with Annexin V/Propidium Iodide

The analysis of the apoptotic *versus* necrotic effect of PVP and citrate-coated AgNP (5, 10 and 50 nm) in human monocytes and macrophages were performed by a flow cytometric annexin V/propidium iodide assay.

The results showed that AgNP significantly induce cell death in both cellular models, in a concentration-dependent manner, independent of the coating agent tested.

Figure 2 shows that, for human monocytes, late apoptosis was only observed for 5, 10 and 50 nm of PVP and citrate-AgNP. In this case, the smaller PVP and citrate-coated AgNP (5 nm) exerted the strongest late apoptotic effects in human monocytes. It is also possible to note that, for citrate-AgNP, the late apoptotic effects were not observed for 10 nm and 50 nm. Contrarily, for the 10 and 50 nm PVP-AgNP, the late apoptotic effects still occurred for the highest concentrations (25 and 12.5 and 25 μg/mL, respectively). No significant effects were observed for Ag^+ and the coating agents, citrate and PVP, per se under the same experimental conditions.

In turn, in macrophages, a peak of early apoptosis followed by late apoptosis induced by PVP and citrate-coated AgNP, 5 and 10 nm were observed (Fig. 3A, B). In fact, in macrophages, early apoptosis and late apoptosis are only induced by smaller AgNP (5 and 10 nm), but not by larger ones (50 nm). Regarding the results presented in Fig. 3A and B, it is possible to verify that the PVP and citrate-coated AgNP induce late apoptotic effects more prominently than early apoptotic effects. In fact, 5 nm PVP-coated AgNP and 10 nm citrate-coated AgNP only exhibited late apoptotic effects. Although there is a tendency for increased early apoptosis with the 10 nm citrate-coated AgNP, this effect has no statistical significance. For 10 nm PVP-coated AgNP, the early and late apoptotic effects are only observed at the maximum concentration tested (25 μg/mL). Oppositely, 5 nm citrate coated-AgNP induced early apoptosis in human macrophages at 12.5

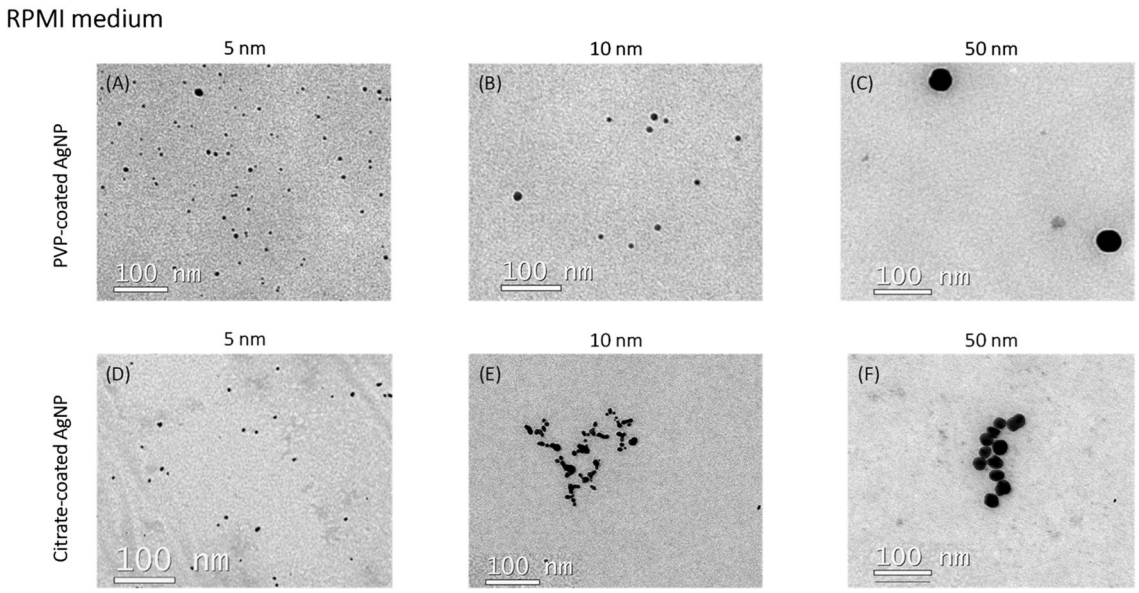

Fig. 1 Characterization, by TEM, of PVP and citrate-coated AgNP (5, 10 and 50 nm) in RPMI medium: 5 nm PVP-AgNP (**A**); 10 nm PVP-AgNP (**B**); 50 nm PVP-AgNP (**C**); 5 nm citrate-AgNP (**D**); 10 nm citrate-AgNP (**E**); 50 nm citrate-AgNP (**F**). Magnification of the TEM images in water: 30 k (c, f), 60 k (b, d, e), 80 k (a); magnification of the TEM images in RPMI: 200 k (a–f)

Table 1 PVP and citrate-coated AgNP size, determined by TEM.

	PVP—AgNP			Citrate—AgNP		
	5 nm	10 nm	50 nm	5 nm	10 nm	50 nm
Water [Size mean ± SD (nm)]	5.4 ± 0.8	10.6 ± 2.1	46 ± 5	5.5 ± 1.0	10.4 ± 2.2	47 ± 5
RPMI medium [Size mean ± SD (nm)]	5.9 ± 1.5	10.9 ± 1.9	48 ± 2	4.5 ± 1.7	10.1 ± 1.5	49 ± 2

The results are expressed as mean value ± standard deviation (SD)

*The TEM data of AgNP characterization in water were kindly provided by the manufacturer, nanoComposix (San Diego, CA)

and 25 µg/mL (Fig. 4A). Regarding the late apoptotic effects, similarly to what occurred in human monocytes, the smaller AgNP exhibited the strongest cytotoxic effects, independent of the coating agent. The 10 nm citrate-coated AgNP did not induced significant late apoptosis in this cellular model.

No significant early apoptotic/ late apoptotic effects were observed for Ag^+ and for the coating agents, citrate and PVP, per se under the same experimental conditions.

Interestingly, a marked necrotic effect was only observed in macrophages treated with the two types of 50 nm AgNP (Fig. 4A, B). At lower concentrations (6.3 µg/mL), the necrotic effect was more noticeable with PVP-coated AgNP than citrate-coated AgNP (Fig. 4A). At the maximum concentration tested (25 µg/mL), the necrotic effect induced by AgNP was similar for the two coating agents (Fig. 4B).

Necrotic and apoptotic effects for Ag^+ and the coating agents, citrate and PVP, were not observed per se under the same experimental conditions.

Considering the necrotic effects of PVP and citrate-coated AgNP (50 nm), measured by annexin V/propidium iodide assay, TEM analysis of cells exposed to this type of AgNP was carried out to examine the morphological modifications. The images acquired are depicted in Fig. 5 and, as it can be observed, in comparison to the unstimulated control, both citrate and PVP coated-AgNP (50 nm) induced significant morphological modifications in human macrophages that are typical of necrosis. Several forms of necrosis were observed with TEM. The macrophages exhibited loss of a distinct (Fig. 5B1, C1) or total loss (Fig. 5B2) of the nuclear envelope, and mitochondria and other organelles were enlarged and swollen, indicating different degrees of necrosis. In both conditions, the presence of lipid droplets, abundance

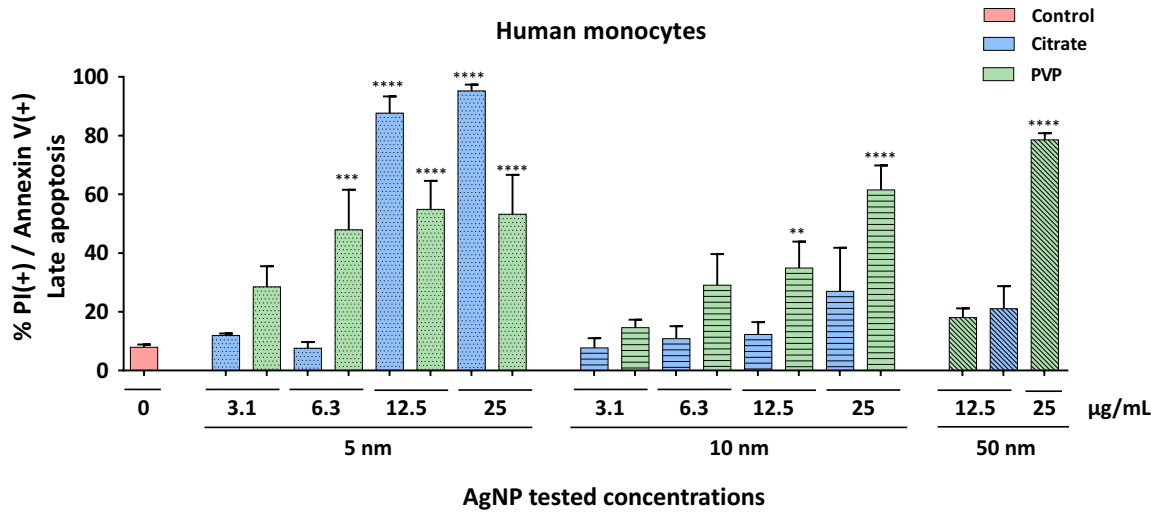

Fig. 2 Late apoptotic effects induced by PVP and citrate-coated AgNP, 5, 10 and 50 nm, in human monocytes, after 2 h of exposure, measured by annexin V/propidium iodide assay. $^{**}P<0.01$, $^{***}P<0.001$, $^{****}P<0.0001$, when compared with the control (untreated cells). Values are presented as the means ± SEM ($n \geq 3$)

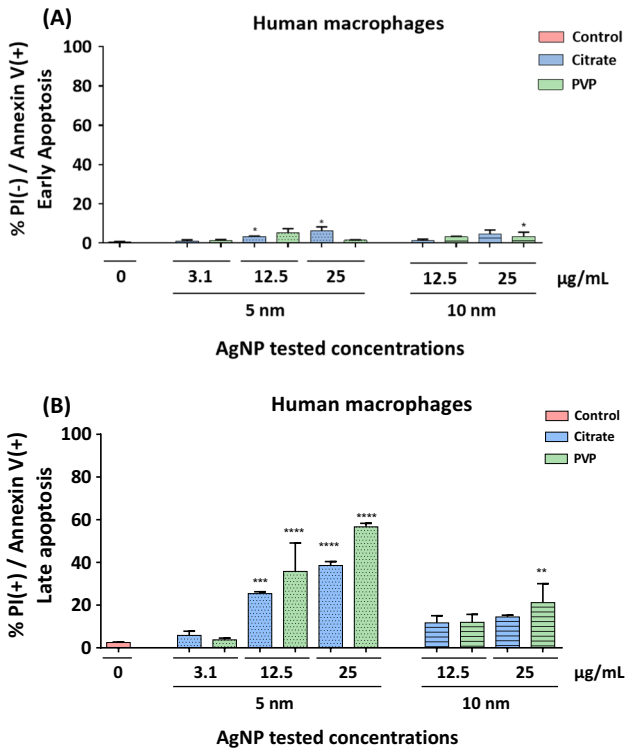

Fig. 3 Early apoptotic **A** and late apoptotic effects **B** induced by PVP and citrate-coated AgNP, 5 and 10 nm, on human macrophages, after 24 h of exposure, measured by annexin V/propidium iodide assay. $^{*}P<0.05$, $^{**}P<0.01$, $^{***}P<0.001$, $^{****}P<0.0001$, when compared with the control (untreated cells). Values are presented as the means ± SEM ($n \geq 3$)

of Golgi apparatus and endoplasmic reticulum, scattered chromatin, and loss of pseudopods (B1, B2) were observed.

Cells show the presence of several autophagic vacuoles of different sizes that enclose cytoplasmic components (B1, C1).

Assessment of mitochondrial membrane potential

It is known that apoptotic processes are closely related to the loss of mitochondrial potential, Δψm. Therefore, to disclose the role of mitochondria in AgNP-induced cell death, the conditions that induced apoptosis in human monocytes [5 nm citrate-coated AgNP (25; 12.5 µg/mL), 5 nm PVP-coated AgNP (25; 12.5; 6.25 µg/mL), 10 nm PVP-coated AgNP (25; 12.5 µg/mL) and 50 nm PVP-coated AgNP (25 µg/mL)] and in macrophages [5 nm citrate-coated AgNP (25; 12.5 µg/mL), 5 nm PVP-coated AgNP (25; 12.5 µg/mL) and 10 nm PVP-coated AgNP (25; 12.5 µg/mL)] were selected to evaluate the depolarization of Δψm, using the JC-1 cationic dye, through flow cytometry.

First, an optimization of the incubation time of the cellular models treated with the positive control (CCCP) was performed. The same incubation periods used for other assays were tested. As monocytes are fresh primary cells, an incubation period of 2 h was sufficient to observe effects on Δψm. However, considering that macrophages are cultured cells, 16 h were the incubation period that originate measurable effects on Δψm. Additionally, 24 h was also tested, but this time exposure induced an excessive Δψm alteration,

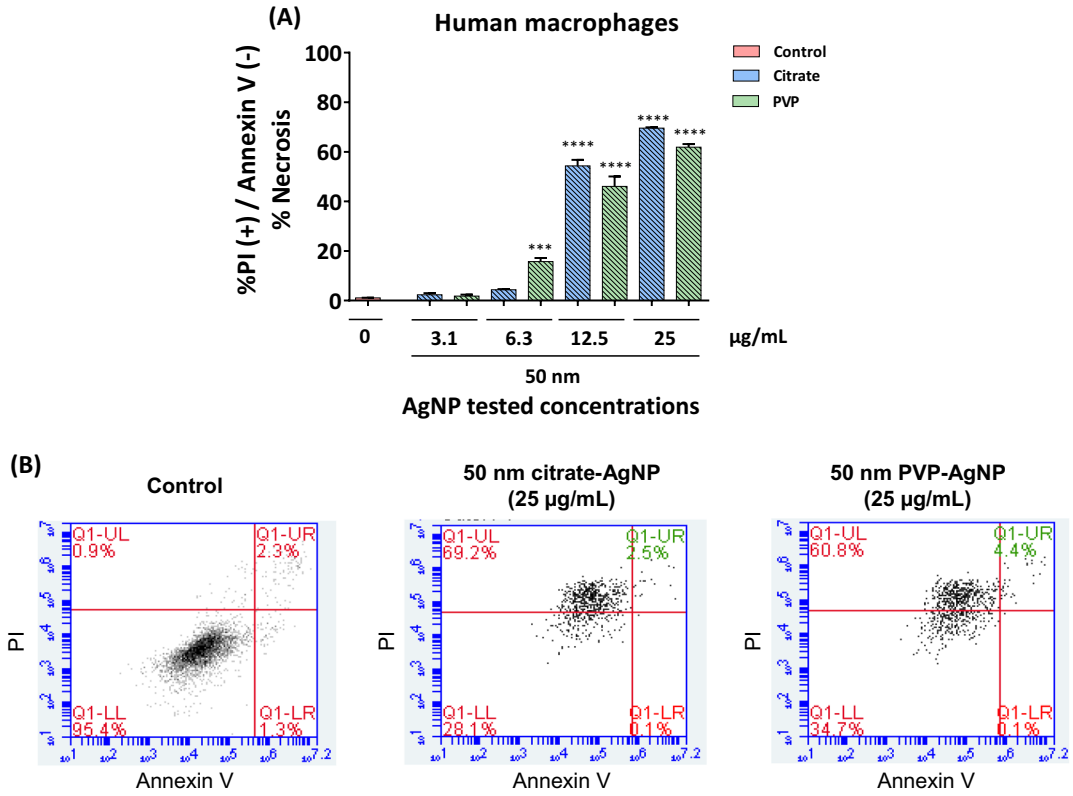

Fig. 4 Necrotic effects of PVP and citrate-coated AgNP (50 nm), induced on macrophages, after 2 h of exposure, measured by annexin V/propidium iodide assay. ***$P<0.001$, ****$P<0.0001$, when compared with the control (untreated cells). Values are presented as the means ± SEM ($n \geq 3$) (**A**). Representative flow cytometry plots of of annexin-V/propidium iodide binding assay for 50 nm PVP and citrate-coated AgNP, for the maximum tested concentration (25 µg/mL) (**B**)

which is the reason why 16 h was selected to perform this assay. Under these experimental conditions, the exposure of macrophages to the above mentioned AgNP did not induce a significant depolarization of Δψm relatively to the untreated control. In contrast, the exposure of human monocytes to PVP and citrate-coated AgNP resulted in a significant depolarization of Δψm, well denoted by the decrease of the reddish fluorescence shifting to an increase in green fluorescence (as seen in FL-1/FL-2 channels ratio), according to Fig. 6B. In fact, as represented in Fig. 6A, for the maximum tested concentration (25 µg/mL), all the tested conditions exhibited an increased depolarization of Δψm (27–30 %), in comparison to the untreated control. In the case of 12.5 µg/mL of 5 nm PVP-coated AgNP, it still induced a strong depolarization of Δψm in human monocytes (Fig. 6A). It was also not observed in a significant % of cells with reduced Δψm when exposed to Ag^+ or coating agents PVP and citrate. As expected, the positive control used, CCCP (0.1–200 µM) induced a concentration-dependent disruption of Δψm, for both cell types.

Detection and quantification of human inflammatory cytokines

The detection and quantification of a set of human inflammatory cytokines (IL-8, IL-1β, IL-6, IL-10, TNF and IL-12p70) were performed in human monocytes and macrophages. Based on the previous cell viability assays, these cells were exclusively stimulated with two concentrations of PVP and citrate-coated AgNP: one that did not cause any effects in the viability of those cellular models (3.1 µg/mL) and one that induced significant effects in their viability (25 µg/mL).

The results obtained for both cellular models are depicted in Fig. 7.

Considering the secretion of the anti-inflammatory cytokine IL-10, for human monocytes, only 5 and 10 nm PVP-coated AgNP increased IL-10 concentration. In macrophages, 5 nm citrate-coated AgNP also significantly increased IL-10 concentration. Apparently, the size did not influence IL-10 secretion, since similar effects were observed for both 5 and 10 nm PVP-AgNP. Nonetheless, the AgNP with the larger size (50 nm) did not lead to differences in IL-10 concentrations, in both cellular models.

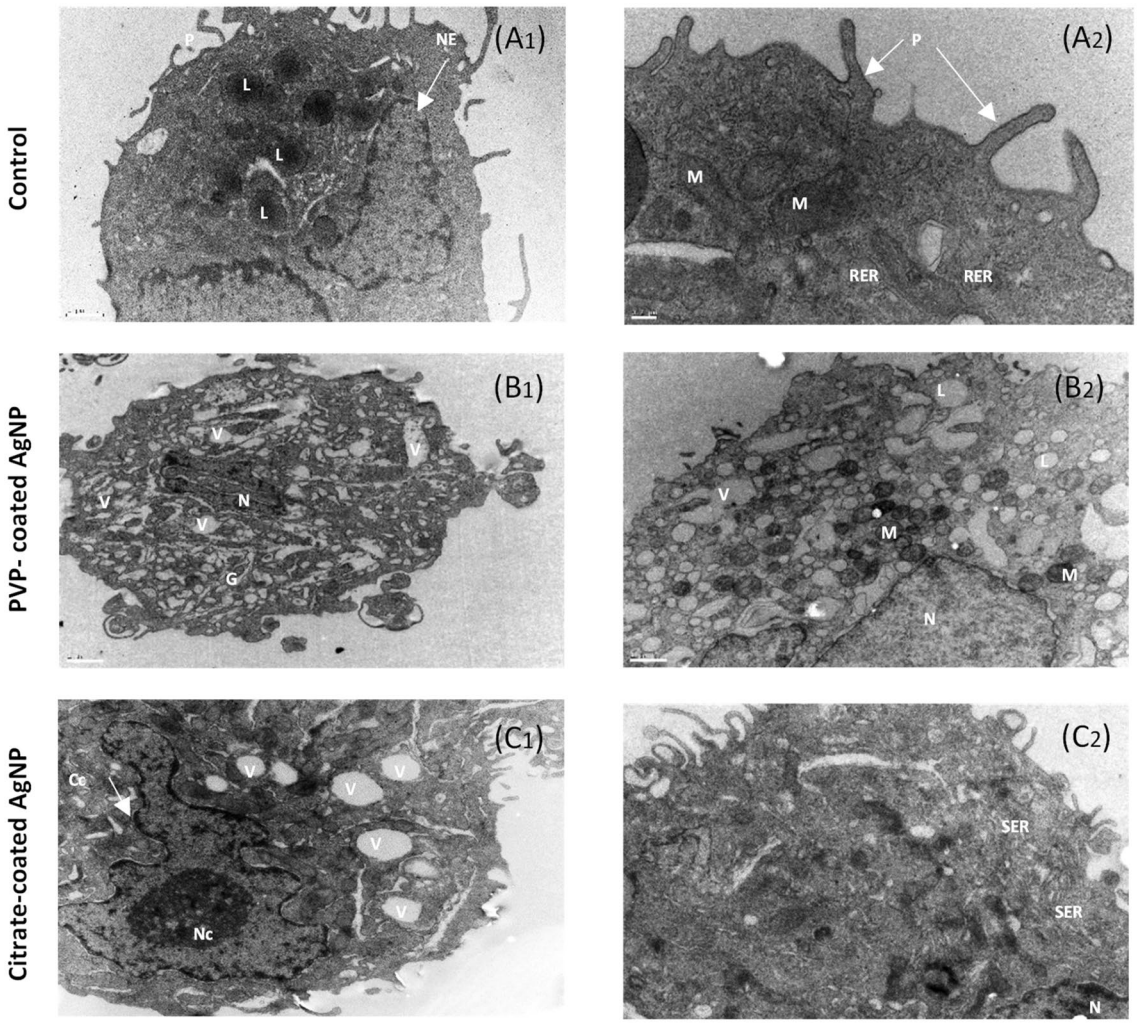

Fig. 5 TEM images of differentiated THP-1 cells: non-treated control (**A1** and **A2**), treated with PVP-coated AgNP (50 nm) (**B1** and **B2**), treated with citrate-coated AgNP (50 nm) (**C1** and **C2**), acquired by JEOL JEM 1400 transmission electron microscope. Magnification of the TEM images: 8 k (b2), 12 k (a1, a2, b1, c1), 40 k (c2). *Cc* condensed chromatin, *G* golgi apparatus, *L* Lipid droplets, *M* mitochondria, *NE* nuclear envelope, *Nc* nucleolus, *N* Nucleus, *P* pseudopods, *RER* Rough endoplasmic reticulum, *SER* smooth endoplasmic reticulum

Regarding the pro-inflammatory cytokine TNF, for 5 nm PVP-coated AgNP, the profile observed for its secretion is the opposite from that observed for macrophages. For monocytes, the lowest concentration of 5 nm PVP-coated AgNP (3.1 µg/mL) and the highest concentration of 10 nm citrate-coated AgNP (25 µg/mL) significantly reduced the TNF secretion, relatively to the untreated control, in human monocytes. Oppositely, in macrophages, only an effect for 5 nm PVP-coated AgNP was observed, at the highest concentration (25 µg/mL) which greatly increased the TNF secretion. Once again, the AgNP with the larger size (50 nm) did not lead to differences in TNF concentrations.

In human monocytes, an increase in IL-8 secretion was observed for lower concentrations of 5 nm PVP and citrate-coated AgNP (3.1 µg/mL). When the stimulus increased to 25 µg/mL, a reversal effect seems to occur as an abrupt decrease in IL-8 secretion was noticed. Oppositely, in macrophages, a concentration-dependent increase in IL-8 concentration of 5 and 10 nm PVP and citrate coated AgNP were observed.

For pro-inflammatory cytokine IL-6, there were no significant effects on its secretion in human monocytes stimulated with AgNP. On the other hand, in macrophages, a concentration-dependent effect was observed when this cellular model was stimulated with 5 nm and 10 nm of PVP and citrate-coated AgNP. PVP-coated AgNP, 50 nm, induced an increase in IL-6 secretion in this cellular model. In this case, the effect depicted seems to be not dependent on size but rather on coating, as there is a more

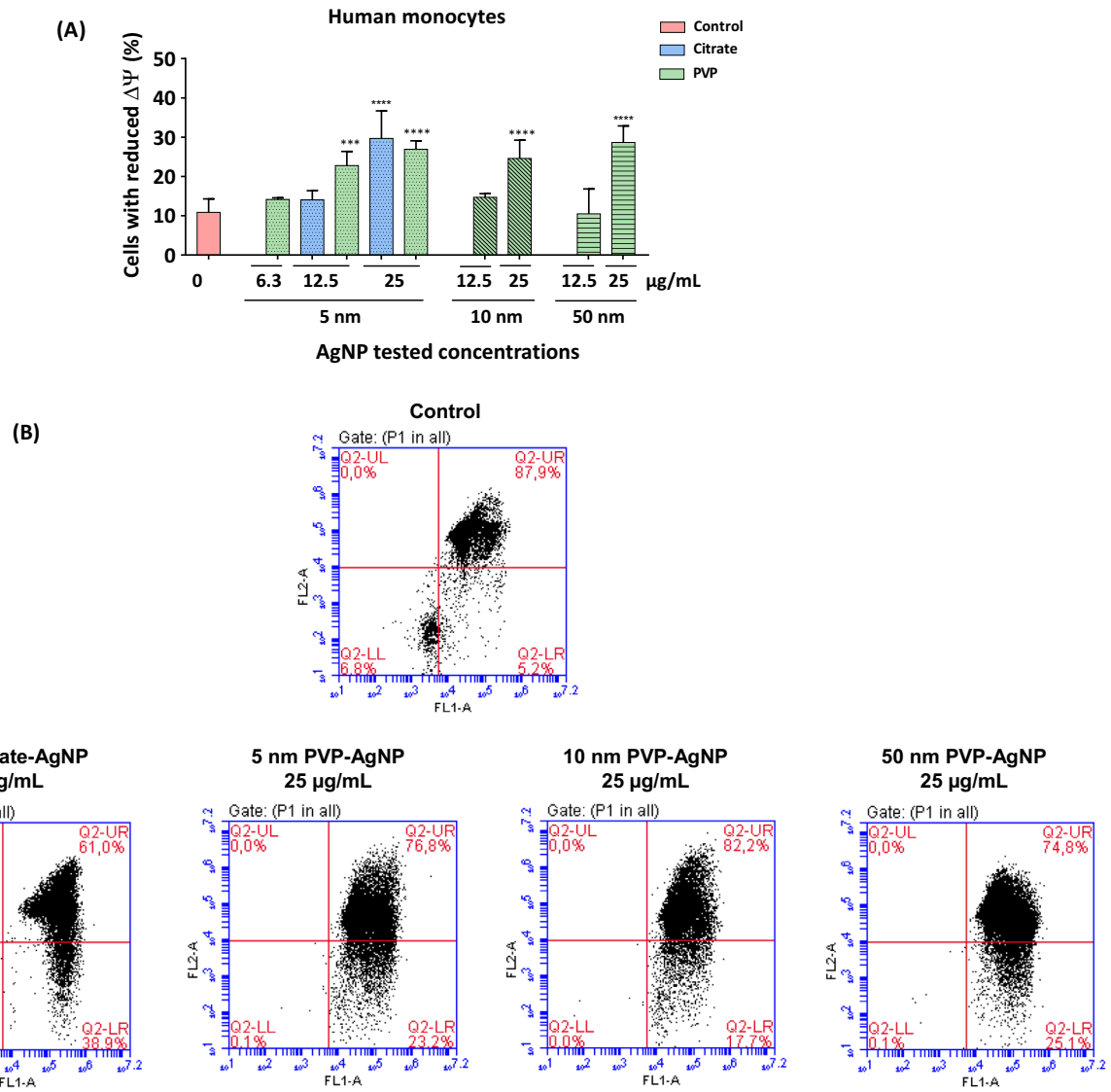

Fig. 6 Effects of PVP and citrate-coated AgNP (0–25 µg/mL) in the alteration on Δψm of human monocytes, assessed by flow cytometric analysis of JC-1 (**A**). Results are expressed as the mean of percentage of cells with Δψm alteration ± SEM ($n \geq 3$). ****$P < 0.0001$, when compared with the control (untreated cells). **B** Representative flow cytometry plots of JC-1 for control, 5 nm citrate-coated AgNP, 5 nm PVP-coated AgNP, 10 nm PVP-coated AgNP, 50 nm PVP-coated AgNP (25 µg/mL)

prominent increase when macrophages were stimulated with PVP-coated AgNP than with citrate-coated AgNP.

The stimulation of both cellular models did not lead to differences in the secretion of the cytokines IL-12 and IL-1β, when compared with control.

Overall, the results of cytokine detection and quantification showed that the effects are more pronounced when both cellular models were treated with smaller AgNP (5 and 10 nm), a more prominent effect with PVP-coated AgNP was also observed.

No effects were observed for Ag^+ (0.25 µg/mL) and the coating agents PVP and citrate (0.01 µg/mL), per se.

Discussion

The present study aimed to fill a gap in literature by disclosing the cytotoxic and pro-inflammatory effects of PVP and citrate-coated (5, 10 and 50 nm) AgNP against cells of innate immune system, namely human monocytes and macrophages, with a specific focus on size and/or coating dependency. The AgNP concentrations used in this study to stimulate monocytes and macrophages (up to 25 µg/mL) were chosen based on previous studies for a possible human long term- exposure or following acute accidental exposure to AgNP (Lee et al. 2012; Wang et al. 2014; Ferdous and Nemmar 2020). Exposure data available from workers in

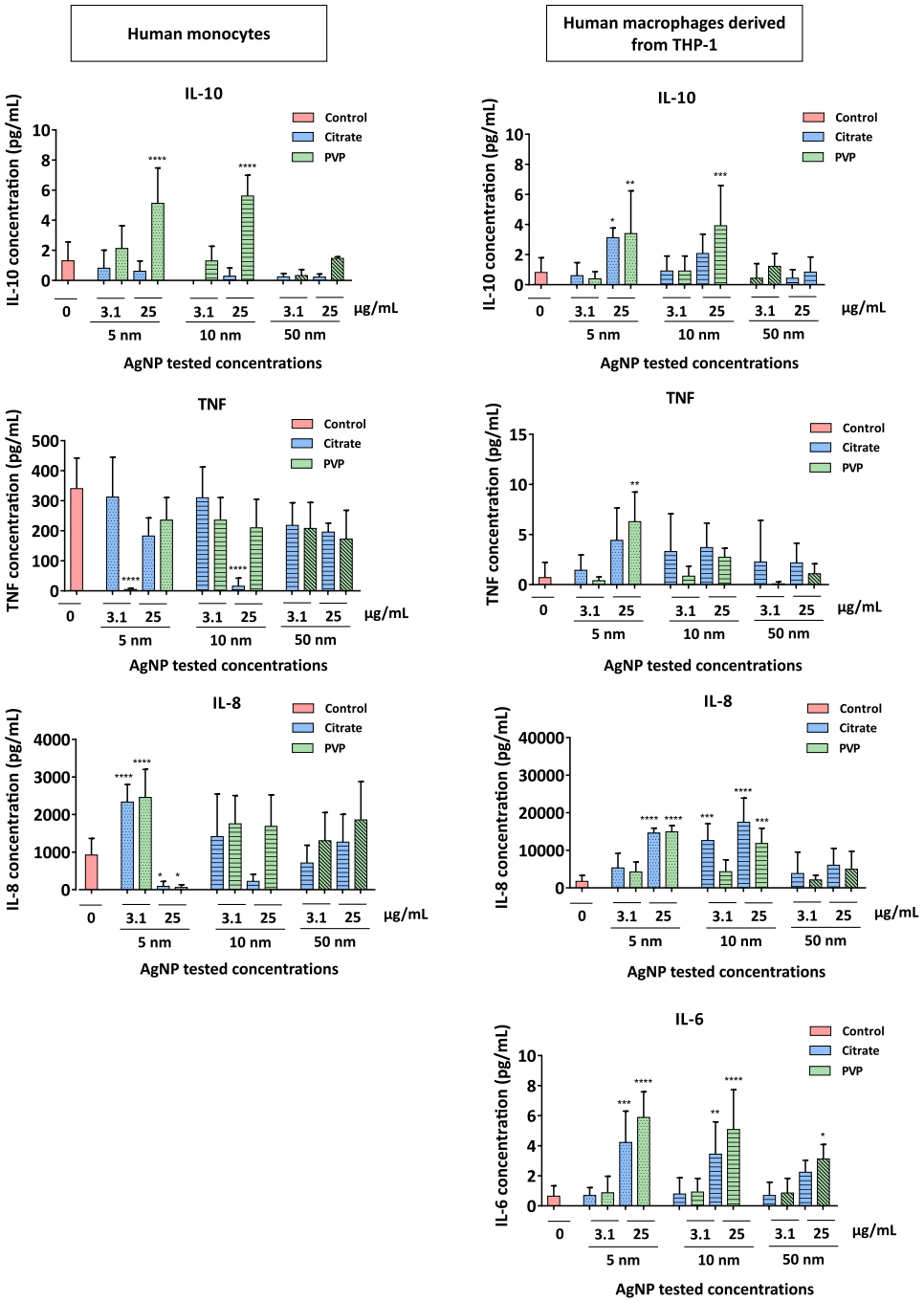

Fig. 7 Cytokine release from human monocytes and macrophages exposed to 5, 10 and 50 nm PVP and citrate-coated AgNP (3.1 and 25 µg/mL). Results, reported as pg/mL of cytokines released in the media, are the mean ± SEM of three independent experiments. *$P < 0.05$, **$P < 0.01$, ***$P < 0.001$, ****$P < 0.0001$, when compared with the control (untreated cells)

an AgNP manufacturing facility indicates that 10 µg/mL of AgNP would approximately correspond to the total cellular deposition following 74 working weeks (8 h per day, 5 days per week) (Gliga et al. 2014). Moreover, it was also considered that the daily acute human ingestion of silver is estimated to be around 20–80 µg (Lee et al. 2012; Wang et al. 2014; Ferdous and Nemmar 2020).

The physicochemical properties of AgNP are very important for their biodistribution, toxicity and efficacy. Thus, their characterization is essential to assess healthy and safety hazards for their possible applications (Barkat et al. 2018; Chugh et al. 2018; Sharma et al. 2019). In this study, AgNP characterization in RPMI culture medium was first performed and were later compared with the data obtained in

the AgNP characterization in water. Despite the complexity of this medium, the results evidenced that, in comparison to water, AgNP of both coatings, in all sizes, maintained their morphology and size, without signs of any significant aggregation, in RPMI medium.

Subsequently, the potential toxicity of AgNP was evaluated in both cellular models. The exposure time of monocytes and macrophages with the nanoparticles used in study was different due to the fact that the monocytes used are fresh cells, isolated daily from human blood, and therefore have a much shorter viability time than the macrophages, which are cultured cells. In addition, these incubation times attempt to mimic what happens in the human body after exposure to an inflammatory stimulus such as AgNP. Through inflammatory stimuli, monocytes move into the bloodstream and remain there for only a few hours before migrating into the tissues, where they differentiate into macrophages. These, in turn, perform more specific functions in the elimination of the inflammatory stimulus, as phagocytosis, and may remain in the tissues for a long time, until the stimulus is completely eliminated.

To ascertain the possible AgNP cytotoxic effects and to better understand what mechanism of cell death is induced by exposure to the AgNP under study, the two cellular models were exposed to AgNP and then were analyzed by a flow cytometric annexin V/propidium iodide assay. For human monocytes, any relevant early apoptotic and necrotic effects were not observed, but the induction of an intermediate state of cellular death, known as late apoptosis was observed. As expected, this effect was induced more exuberantly for the smaller AgNP (5 nm), for both coatings. In larger sizes (10 and 50 nm), the late apoptotic effect was still induced for PVP-coated AgNP. Therefore, it can be assumed that 5 nm PVP-coated AgNP are most cytotoxic to human monocytes since these can overcome cell entrance barriers and are able to pass through cell membranes by direct translocation and/or through phagocytosis. The smaller AgNP also have a larger specific surface area, being more available to interact with cellular components (nucleic acids, fatty acids, proteins, carbohydrates) and, therefore, to exert cytotoxicity (Huang et al. 2017). For macrophages, it seems that the cellular death is induced by AgNP in a slightly different way than with monocytes, as it was observed the occurrence of the three mechanisms of cellular death: early apoptosis, late apoptosis and necrosis. While early apoptosis and late apoptosis were observed for the smaller sizes of PVP and citrate-coated AgNP (5 and 10 nm), necrosis was only observed for the PVP and citrate-coated AgNP of 50 nm. Similarly to what occurred in human monocytes, the apoptotic effects in macrophages were dependent not only on the AgNP concentration, but also on AgNP' size and coating. The apoptotic and late apoptotic effects were more significantly induced by smaller AgNP (5 nm), coated with PVP. Under these experimental conditions, PVP-AgNP also seemed to be more cytotoxic to macrophages, since these triggered a potent necrotic effect, even at low concentrations (6.3 µg/mL). These results suggest that the smaller AgNP, are easily taken into both cell types, which contribute to activate pro-apoptotic cascades. Nevertheless, the larger ones only produced effects in macrophages. These cells are able to phagocytize particles with higher dimensions, which may explain the observed effects. There are few studies in the literature exploring the dependence of the cytotoxic effects of AgNP in terms of size and coatings and particularly on human immune cells. A previous work from our group, Freitas et al. (Freitas et al. 2008), in which the effects of 5, 10 and 50 nm PVP and citrate-coated AgNP against human neutrophils were explored, showed cytotoxic effects of AgNP dependent on concentration, size and coating (Freitas et al. 2008). It was found that, in neutrophils, 5 nm citrate-coated AgNP (25 µg/mL) induced a significant cell death (Freitas et al. 2008). Concerning the type of cell death induced by AgNP, the authors did not observe significant apoptotic effects in human neutrophils (Freitas et al. 2008). Even though neutrophils, monocytes and macrophages are immune cells that can phagocytose and destroy infectious agents, it is known that the first cells to reach inflammatory sites are neutrophils. After this first-line defense, the monocytes are then mobilized from blood to the inflammatory site as a second-line defense, generating proinflammatory mediators as cytokines (IL-6, TNF, IL-1) to attract monocytes and lymphocytes, being also able to differentiate into macrophages for the resolution of the inflammatory response (Kantari et al. 2008). Therefore, the different roles of these three types of cells in the course of an inflammatory response, results in different responses and resistance to a pro-inflammatory foreign agent, which could explain the differences found between these studies. Another study, carried out by our group, Soares et al. (Soares et al. 2016), in which the effect of the size of PVP-AgNP in human neutrophils was studied, corroborate the conclusions of the present work. The authors showed that smaller AgNP (10 nm) exhibit more toxicity than the larger ones (50 nm). This conclusion was based on the analysis of human neutrophils viability when these were incubated with 10 nm and 50 nm AgNP, by the PI staining method, where a considerable increase of necrotic cells was observed when they were exposed to the smaller AgNP (Soares et al. 2016). Available data also show that, in rat alveolar macrophages, RAW 264.7, alveolar macrophages cells, exposed to different AgNP sizes (15–113 nm), smaller AgNP induced significant cytotoxic effects when compared with the other tested sizes (Carlson et al. 2008; Park et al. 2010).

Mitochondria play a crucial role in the immune system, particularly in regulating the responses of immune cells to tissue injury, pathogens or foreign stimuli, and inflammation

(Maurer and Meyer 2016; West and Shadel 2017; Faas and de Vos 2020). In fact, the reduced Δψm is considered as an initial and irreversible step towards apoptosis. The energy released during the oxidation reactions in the mitochondrial respiratory chain is stored as a negative electrochemical gradient across the mitochondrial membrane and the Δψm is referred to as being polarized. The collapse of the Δψm results in a depolarized Δψ, and is often observed to occur early during apoptosis (Webster 2012; Faas and de Vos 2020). Therefore, to disclose the role of mitochondria in AgNP-induced cell death by apoptosis, the depolarization of Δψm in both cellular models after exposure to AgNP in the conditions that induced cell death by apoptosis was evaluated. Irrespective of the AgNP coating, our results evidenced a non-significant depolarization of Δψm of macrophages. Nonetheless, the human monocytes exhibited an exuberant depolarization of Δψm in a concentration-dependent manner, in comparison to the untreated control, for both AgNP coatings. Based on these findings, it can be stated that the induction of apoptosis in human monocytes exposed to AgNP, occurs as a result of mitochondrial damage with consequent alterations of Δψm, independently of size and coating. The direct or indirect interaction of AgNP with mitochondria of immune cells are not yet fully understood, as there are only a few studies in the literature exploring this effect, of which only one was carried out in human cells. Orlowski et al. (Orlowski et al. 2013) studied the effects of tannic acid-coated AgNP, with different sizes (13, 33, 46 nm), using mouse Raw 264.7 monocytes. The authors also observed that the alterations of Δψm induced by AgNP was directly proportional to the increasing concentrations of AgNP and that the smaller AgNP sizes induced more cytotoxic effects (Orlowski et al. 2013). In agreement to our results, Vuković et al. (Vuković et al. 2020) also observed the depolarization of mitochondrial membrane after the exposure of circulating human peripheral blood mononuclear cells (hPBMC) to 10 nm PVP-AgNP, in a concentration dependent manner, even after a short period of exposure (1 h) (Vuković et al. 2020). Aude-Garcia et al. (Aude-Garcia et al. 2016) also measured the influence of PVP-coated AgNP (25–100 nm) in the mitochondrial function of bone-marrow derived macrophages from C57BL/6 and verified that acute exposure to AgNP induced an important decrease in the transmembrane Δψm.

The exposure of immune cells to xenobiotics is associated with the occurrence of several pro-inflammatory mechanisms, including the production of pro-inflammatory cytokines (Kim and Choi 2012; Gustafson et al. 2015; Akter et al. 2018; Ninan et al. 2020). During the course of an inflammatory response, monocytes and macrophages are considered the main producers of inflammatory and immunoregulatory cytokines (Kantari et al. 2008; Kany et al. 2019). Therefore, in our work, the influence of the exposure of PVP and citrate-coated AgNP (5, 10 and 50 nm) in the release of cytokines by human monocytes and macrophages was assessed. The results evidenced that human monocytes seemed to be more sensitive to AgNP exposure than macrophages, since an increased production of TNF and IL-8 secretion was only found for monocytes. Surprisingly, an exposure of human monocytes to the highest concentration (25 μg/mL) of PVP and citrate coated-AgNP of 5 and 10 nm, resulted in an abrupt decrease of the release of pro-inflammatory cytokines TNF and IL-8, in comparison to the control. Considering the potent cytotoxic effects observed on viability and even the alterations of the Δψm induced by higher concentrations of AgNP, it can be assumed that the lower metabolic state of the cells, in these experimental conditions, compromised their production of TNF and IL-8. The greater sensitivity of monocytes to AgNP exposure is notorious, since low concentrations (3.1 μg/mL) are sufficient to activate these cells and induce a higher IL-8 production, a chemotactic factor for neutrophils and lymphocytes during an inflammatory response (Brennan and Zheng 2007). In opposition to the results observed for human monocytes, macrophages appear to be more resistant to the lower sizes (5, 10 nm) of PVP and citrate-coated AgNP exposure, presenting an increased secretion of TNF, IL-8 and IL-6 observable for the higher concentrations (25 μg/mL) but not for the lower ones (3.1 μg/mL). Although macrophages also suffer a reduction on their viability upon exposure to AgNP, this reduction is less pronounced than in monocytes, explaining the production of pro-inflammatory cytokines. The increase of these cytokines also reveals that macrophage response to AgNP is mainly characterized by the orchestration of the production of several other pro-inflammatory cytokines and the recruitment, differentiation and activation of other immune cells to the resolution of the inflammatory response. In general, it is possible to assume that macrophages induce a more pronounced response after exposure to AgNP, especially the smallest ones (5 nm) coated by PVP.

Interestingly, the results also evidenced a significant production of IL-10, in both cellular models, for the smaller PVP and citrate-coated AgNP (25 μg/mL). Considering the anti-inflammatory nature of IL-10, it can be inferred that, upon contact of the immune system with AgNP, a pro-inflammatory response is triggered and, to prevent this response from becoming too prolonged and contributing to a state of chronic inflammation, the immune system provides a negative feedback to dampen the magnitude of immune responses, through the release of anti-inflammatory factors such as IL-10, limiting in this way the cellular damage induced by AgNP. This defensive behavior of immune cells, especially monocytes and macrophages, during the course of an inflammatory response with other foreign stimuli is already described in the literature (Byrne and Reen 2002; Standiford and Deng 2006; Staples et al. 2007; Couper et al. 2008; Shouval et al. 2014; Morhardt et al. 2019). However,

considering the effects induced by AgNP in cell viability, our results suggest that the contact of AgNP with immune cells is so deleterious that it surpasses the anti-inflammatory activity of IL-10, since an increased release of pro-inflammatory cytokines was observed which culminate in cell death. Although there are no studies in the literature exploring the effect of various AgNP sizes and coatings on immune cells, there are already some studies showing that the exposure of these cells to AgNP leads to increased cytokine production. Murphy and colleagues (Murphy et al. 2016) investigated the ability of PVP-AgNP (< 100 nm) to induce a response in a monocyte cell line, more precisely, the transcription and release of IL-1, IL-6, TNF and IL-1β. These authors observed that the exposure to AgNP resulted in up-regulation of inflammatory cytokines IL-1, IL-6 and TNF in THP-1 cells and primary human monocytes (Murphy et al. 2016). Yang and colleagues (Yang et al. 2012) also studied the effects of PVP-coated AgNP (5, 28 and 100 nm) and demonstrated that smaller PVP-coated AgNP (5 nm) induced the production of IL-1β in human peripheral blood mononuclear cells (PBMCs) and primary monocytes, evidencing their critical role in initiating the innate immune response and also regulating the adaptive immunity. Orlowski et al. (Orlowski et al. 2013) assessed the response of monocytes to AgNP (10–65 nm). Similarly to what was observed in this study, the authors observed a strong down-regulation of the production of TNF by monocytes, while no significant effects were observed for the other cytokines (IL-6, IL-10, IFN-γ and IL-12p70) (Orlowski et al. 2013). Nevertheless, there are some studies that did not evidence an increase in cytokines upon the exposure of immune cells to AgNP. This is the case of Haase et al. (Haase et al. 2014), who evaluated the impact of AgNP (2.0–34.7 nm) on the expression of TNF promoter in Raw 264.7 cells and Parnsamut and Brimson (Parnsamut and Brimson 2015), who investigated the effect of PVP and sodium citrate-coated AgNP (10–50 nm) on IL-2, IL-6 and TNF in monocytic U937 cells did not observe any significant differences induced by AgNP. Despite the controversial results in the literature (due to differences in cell type, different types AgNP and detection methods), it can be inferred that the cytotoxic action of AgNP may also be due to their interference in of the production of pro- and anti-inflammatory cytokines.

Conclusions

From the results obtained in this study, it can be inferred that AgNP exert toxic effects in human monocytes and macrophages. This cytotoxic action is probably triggered trough the activation of these cells and, consequently, the initiation of an inflammatory response that is mainly associated with the disruption of $\Delta\psi m$ and the release of pro-inflammatory cytokines, culminating in the decrease of viability of immune cells. This study also evidenced that the cytotoxic effects of AgNP vary according to their physicochemical properties, namely their size and coating. In fact, the smaller AgNP exhibited more cytotoxic effects in human monocytes and macrophages. Concerning the coating agent, PVP-coated AgNP depicted more harmful effects in human monocytes and macrophages than citrate-coated AgNP. The findings of the present study provide new insight into the interaction AgNP with the cells of the immune system. Considering the increased daily use of AgNP, it is imperative to further explore the adverse outcomes and mechanistic pathways leading to AgNP-induced pro-inflammatory effects to deep insight into the molecular mechanism involved in this effect.

Acknowledgements The authors gratefully acknowledge the medical and the nursing staff of the Centro Hospitalar do Porto-Hospital de Santo António Blood Bank for their collaboration in the recruitment of blood donors to participate in the study.

Funding The present work was supported with funding from FCT/MCTES through national funds and 'Programa Operacional Competitividade e Internacionalização (COMPETE) (PTDC/NAN-MAT/29248/2017-POCI-01-0145-FEDER-029248). Adelaide Sousa thanks FCT (Fundação para a Ciência e Tecnologia) and ESF (European Social Fund) through POCH (Programa Operacional Capital Humano) for her PhD grant reference SFRH/BD/150656/2020. Ana T Rufino acknowledges her researcher contract to FCT under the project PTDC/MED-QUI/29243/201 Marisa Freitas acknowledges her contract under the Scientific Employment Stimulus—Individual Call (CEEC Individual) 2020.04126.CEECIND. Marisa Freitas also thanks LAQV-REQUIMTE for her contract under the reference LA/P/0008/2020. The authors acknowledge the support of the i3S Scientific Platform HEMS, member of the national infrastructure PPBI - Portuguese Platform of Bioimaging (PPBI-POCI-01-0145-FEDER-022122).

Data availability The datasets generated during and/or analysed during the current study are available from the corresponding author on reasonable request.

Declarations

Conflict of interest The authors declare that they have no conflict of interest.

Ethical approval All patient-related procedures and protocols were performed in accordance with the Declaration of Helsinki and approved by the Ethics Committee of Centro Hospitalar do Porto. Written informed consent was obtained from all participants.

Consent to participate Written informed consent was obtained from all participants.

References

Akter M, Sikder MT, Rahman MM, Ullah A, Hossain KFB, Banik S, Hosokawa T, Saito T, Kurasaki M (2018) A systematic review on silver nanoparticles-induced cytotoxicity: physicochemical properties and perspectives. J Adv Res 9:1–16

Arora S, Rajwade JM, Paknikar KM (2012) Nanotoxicology and in vitro studies: the need of the hour. Toxicol Appl Pharmacol 258(2):151–165

Aude-Garcia C, Villiers F, Collin-Faure V, Pernet-Gallay K, Jouneau PH, Sorieul S, Mure G, Gerdil A, Herlin-Boime N, Carrière M, Rabilloud T (2016) Different in vitro exposure regimens of murine primary macrophages to silver nanoparticles induce different fates of nanoparticles and different toxicological and functional consequences. Nanotoxicology 10(5):586–596

Barkat MA, Beg S, Naim M, Pottoo FH, Singh SP, Ahmad FJ (2018) Current progress in synthesis, characterization and applications of silver nanoparticles: precepts and prospects. Recent Pat Anti-Infect Drug Discov 13(1):53–69

Berekaa MM (2015) Nanotechnology in food industry; advances in food processing, packaging and food safety. Int J Curr Microbiol App Sci 4(5):345–357

Brennan, K. and J. Zheng (2007). Interleukin 8. xPharm: The Comprehensive Pharmacology Reference. S. J. Enna and D. B. Bylund. New York, Elsevier**:** 1–4

Byrne A, Reen DJ (2002) Lipopolysaccharide Induces Rapid Production of IL-10 by Monocytes in the presence of apoptotic neutrophils. J Immunol 168(4):1968–1977

Carlson C, Hussain SM, Schrand AM, Braydich-Stolle LK, Hess KL, Jones RL, Schlager JJ (2008) Unique Cellular Interaction of Silver Nanoparticles: Size-Dependent Generation of Reactive Oxygen Species. J Phys Chem B 112(43):13608–13619

Chan LL-Y, Kuksin D, Laverty DJ, Saldi S, Qiu J (2015) Morphological observation and analysis using automated image cytometry for the comparison of trypan blue and fluorescence-based viability detection method. Cytotechnology 67(3):461–473

Chiu S, Bharat A (2016) Role of monocytes and macrophages in regulating immune response following lung transplantation. Curr Opin Organ Transplant 21(3):239–245

Chugh H, Sood D, Chandra I, Tomar V, Dhawan G, Chandra R (2018) Role of gold and silver nanoparticles in cancer nano-medicine. Artif Cells Nanomed Biotechnol 46(sup1):1210–1220

Council ER (2012) The Nanodatabase. Retrieved 16 April 2020, from http://nanodb.dk/en/

Couper KN, Blount DG, Riley EM (2008) IL-10: the master regulator of immunity to infection. J Immunol 180(9):5771–5777

de Lima R, Seabra AB, Durán N (2012) Silver nanoparticles: a brief review of cytotoxicity and genotoxicity of chemically and biogenically synthesized nanoparticles. J Appl Toxicol 32(11):867–879

Ducheyne P (2017) Comprehensive biomaterials II. Elsevier, Amsterdam

Faas MM, de Vos P (2020) Mitochondrial function in immune cells in health and disease. Biochim Biophys Acta Mol Basis Dis 1866(10):165845

Fauss E (2008) The silver nanotechnology commercial inventory. University of Virginia, Charlottesville

Ferdous Z, Nemmar A (2020) Health Impact of Silver Nanoparticles: A Review of the Biodistribution and Toxicity Following Various Routes of Exposure. Int J Mol Sci 21(7):2375

Freitas M, Porto G, Lima JLFC, Fernandes E (2008) Isolation and activation of human neutrophils *in vitro*. The importance of the anticoagulant used during blood collection. Clin Biochem 41(7):570–575

Freitas M, Lucas M, Sousa A, Soares T, Ribeiro D, Carvalho F, Fernandes E (2020) Small-size silver nanoparticles stimulate neutrophil oxidative burst through an increase of intracellular calcium levels. World Acad Sci J 2(3):1

Galdiero S, Falanga A, Vitiello M, Cantisani M, Marra V, Galdiero M (2011) Silver nanoparticles as potential antiviral agents. Molecules 16(10):8894–8918

Gliga AR, Skoglund S, Wallinder IO, Fadeel B, Karlsson HL (2014) Size-dependent cytotoxicity of silver nanoparticles in human lung cells: the role of cellular uptake, agglomeration and Ag release. Part Fibre Toxicol 11:11

Gustafson HH, Holt-Casper D, Grainger DW, Ghandehari H (2015) Nanoparticle uptake: the phagocyte problem. Nano Today 10(4):487–510

Haase H, Fahmi A, Mahltig B (2014) Impact of silver nanoparticles and silver ions on innate immune cells. J Biomed Nanotechnol 10(6):1146–1156

(HERO), U. S. E. P. A. H. E. R. O. (2022). "Silver or silver nanoparticles: A hazardous threat to the environment and human health?". Retrieved 15/07/2022, from https://hero.epa.gov/hero/index.cfm/reference/details/reference_id/195554

Huang Y-W, Cambre M, Lee H-J (2017) The toxicity of nanoparticles depends on multiple molecular and physicochemical mechanisms. Int J Mol Sci 18(12):2702

Kantari C, Pederzoli-Ribeil M, Witko-Sarsat V (2008) The role of neutrophils and monocytes in innate immunity. Contrib Microbiol 15:118–146

Kany S, Vollrath JT, Relja B (2019) Cytokines in inflammatory disease. Int J Mol Sci 20(23):6008

Kim S, Choi I-H (2012) Phagocytosis and endocytosis of silver nanoparticles induce interleukin-8 production in human macrophages. Yonsei Med J 53(3):654

Kononenko V, Narat M, Drobne D (2015) Nanoparticle interaction with the immune system/Interakcije nanodelcev z imunskim sistemom. Arch Ind Hyg Toxicol 66(2):97–108

Lai CY, Tseng PC, Chen CL, Satria RD, Wang YT, Lin CF (2021) Different Induction of PD-L1 (CD274) and PD-1 (CD279) Expression in THP-1-Differentiated Types 1 and 2 Macrophages. J Inflamm Res 14:5241–5249

Lee JH, Ahn K, Kim SM, Jeon KS, Lee JS, Yu IJ (2012) Continuous 3-day exposure assessment of workplace manufacturing silver nanoparticles. J Nanopart Res 14:1134

Martirosyan A, Polet M, Bazes A, Sergent T (2012) Food nanoparticles and intestinal inflammation: a real risk? Inflamm Bowel Dis 5:259–282

Mathur P, Jha S, Ramteke S, Jain NK (2018) Pharmaceutical aspects of silver nanoparticles. Artif Cells Nanomed Biotechnol 46(sup1):115–126

Maurer L, Meyer J (2016) A systematic review of evidence for silver nanoparticle-induced mitochondrial toxicity. Environ Sci Nano 3(2):311–322

McClements DJ, Xiao H (2017) Is nano safe in foods? Establishing the factors impacting the gastrointestinal fate and toxicity of organic and inorganic food-grade nanoparticles. Sci Food 1(1):6

Mittar D, Paramban R, McIntyre C (2011) Flow cytometry and high-content imaging to identify markers of monocyte-macrophage differentiation. BD Biosci 1:1–20

Morhardt TL, Hayashi A, Ochi T, Quirós M, Kitamoto S, Nagao-Kitamoto H, Kuffa P, Atarashi K, Honda K, Kao JY, Nusrat A, Kamada N (2019) IL-10 produced by macrophages regulates epithelial integrity in the small intestine. Sci Rep 9(1):1223

Murphy A, Casey A, Byrne G, Chambers G, Howe O (2016) Silver nanoparticles induce pro-inflammatory gene expression and inflammasome activation in human monocytes. J Appl Toxicol 36(10):1311–1320

NanoComposix. (2004). Silver nanoparticles surfaces. Retrieved 09/06/2020, from https://nanocomposix.com/pages/nanocomposix-university#surfaces

Ninan N, Goswami N, Vasilev K (2020) The impact of engineered silver nanomaterials on the immune system. Nanomaterials 10(5):967

Orlowski P, Krzyzowska M, Zdanowski R, Winnicka A, Nowakowska J, Stankiewicz W, Tomaszewska E, Celichowski G, Grobelny J (2013) Assessment of in vitro cellular responses of monocytes and keratinocytes to tannic acid modified silver nanoparticles. Toxicol in Vitro 27(6):1798–1808

Ozleyen A, Yilmaz YB, Tumer TB (2021) Dataset on the differentiation of THP-1 monocytes to LPS inducible adherent macrophages and their capacity for NO/iNOS signaling. Data Brief 35:106786

Parameswaran N, Patial S (2010) Tumor necrosis factor-α signaling in macrophages. Crit Rev Eukaryot Gene Expr 20(2):87–103

Park E-J, Yi J, Kim Y, Choi K, Park K (2010) Silver nanoparticles induce cytotoxicity by a Trojan-horse type mechanism. Toxicol in Vitro 24(3):872–878

Parnsamut C, Brimson S (2015) Effects of silver nanoparticles and gold nanoparticles on IL-2, IL-6, and TNF-α production via MAPK pathway in leukemic cell lines. Genet Mol Res J 14(2):3650–3668

Pathakoti K, Manubolu M, Hwang H-M (2017) Nanostructures: current uses and future applications in food science. J Food Drug Anal 25(2):245–253

Sharma S, Jaiswal S, Duffy B, Jaiswal AK (2019) Nanostructured materials for food applications: spectroscopy, microscopy and physical properties. Bioengineering 6(1):26

Shouval DS, Ouahed J, Biswas A, Goettel JA, Horwitz BH, Klein C, Muise AM, Snapper SB (2014) Chapter Five - interleukin 10 receptor signaling: master regulator of intestinal mucosal homeostasis in mice and humans. Adv Immunol 122:177–210

Soares T, Ribeiro D, Proença C, Chisté RC, Fernandes E, Freitas M (2016) Size-dependent cytotoxicity of silver nanoparticles in human neutrophils assessed by multiple analytical approaches. Life Sci 145:247–254

Standiford TJ, Deng JC (2006). In: Laurent GJ, Shapiro SD (eds) Encyclopedia of respiratory medicine. Academic Press, Oxford, pp 373–377

Staples KJ, Smallie T, Williams LM, Foey A, Burke B, Foxwell BMJ, Ziegler-Heitbrock L (2007) IL-10 induces IL-10 in primary human monocyte-derived macrophages via the transcription factor stat3. J Immunol 178(8):4779–4785

Tanaka T, Narazaki M, Kishimoto T (2014) IL-6 in inflammation, immunity, and disease. Cold Spring Harb Perspect Biol 6(10):a016295–a016295

Vuković B, Milić M, Dobrošević B, Milić M, Ilić K, Pavičić I, Šerić V, Vrček IV (2020) Surface stabilization affects toxicity of silver nanoparticles in human peripheral blood mononuclear cells. Nanomaterials 10(7):1390

Wang X, Ji Z, Chang CH, Zhang H, Wang M, Liao Y-P, Lin S, Meng H, Li R, Sun B, Winkle LV, Pinkerton KE, Zink JI, Xia T, Nel AE (2014) Use of coated silver nanoparticles to understand the relationship of particle dissolution and bioavailability to cell and lung toxicological potential. Small 10(2):385–398

Webster KA (2012) Mitochondrial membrane permeabilization and cell death during myocardial infarction: roles of calcium and reactive oxygen species. Future Cardiol 8(6):863–884

West AP, Shadel GS (2017) Mitochondrial DNA in innate immune responses and inflammatory pathology. Nat Rev Immunol 17(6):363–375

Yang EJ, Kim S, Kim JS, Choi IH (2012) Inflammasome formation and IL-1β release by human blood monocytes in response to silver nanoparticles. Biomaterials 33(28):6858–6867

Zorraquín-Peña I, Cueva C, Bartolomé B, Moreno-Arribas MV (2020) Silver nanoparticles against foodborne bacteria. Effects at intestinal level and health limitations. Microorganisms 8(1):E132